

V_{s30} of Coastal Cities in Eastern Indonesia in the Context of Earthquake Phenomenology

Claire Ashcraft¹, Ron Harris (b) ¹, Julian Fretha², Abby Mangum¹, John McBride (b) ¹, Carolus Prasetyadi³, Kevin Rey (b) ¹, Shayna Orme (b) ¹, Hanif Sulaeman⁴, Diannitta Agustinawati⁵, Bryce Berrett⁶, Rachel Willmore¹, Ethan Westfall¹, Ian Bell¹, Giovani Cynthia Pradipta⁷, Emma Baginski (b) ¹

¹Department of Geological Sciences, Brigham Young University, Provo, Utah, USA, ²Badan Nasional Penanggulangan Bencana (BNPB), Ambon, Indonesia, ³Faculty of Mineral Technology, Universitas Pembangunan Nasional, Jogjakarta, Indonesia, ⁴U-INSPIRE Indonesia, Kelurahan Tegalega, Bogor, Indonesia, ⁵Badan Nasional Penanggulangan Bencana (BNPB), Pacitan, Indonesia, ⁶School of Civil and Construction Engineering, Oregon State University, Corvallis, Oregon, USA, ⁷Faculty of Earth Sciences and Technology, Institut Teknologi Bandung, Indonesia

Author contributions: Conceptualization, Formal Analysis: Ron Harris, Claire Ashcraft. Methodology: All authors. Writing - Original draft: Claire Ashcraft. Writing - Review & Editing: Shayna Orme, Ron Harris, John McBride, Emma Baginski. Technical Expertise: Geophysics: John McBride, Kevin Rey. Engineering Expertise: Bryce Berrett. Field Expedition: Pacitan: Carolus Prasetyadi, Diannitta Agustinawati. Field Expedition: Ambon; MMI Map 2019 Earthquake: Julian Fretha. Translation; MMI Map 1898 Earthquake: Abby Mangam.

Abstract Shear wave velocity measurements to 30 m depth (V_{s30}) using Multichannel Analysis of Surface Waves (MASW) indicate high seismic risk to the built environment in coastal cities adjacent to the Sunda and Banda subduction zones in Eastern Indonesia. These measurements were taken at 58 sites in the cities of Pacitan (southern Java), Lombok, Ambon, and the Banda Islands. Comparing V_{s30} estimates with local geologic maps show low velocities associated mostly with unconsolidated alluvium on coastal plains where most of the built environment resides. Due to recent destructive earthquakes in two of the sites (2018 Lombok and 2019 Ambon) we were able to directly compare damage using the MMI scale to V_{s30} . In most cases the heavy damage was experienced in sites with low V_{s30} values. The least damage was experienced near sites with high V_{s30} values, which are in foothills underlain by shallow volcanic units. These data provide a way to quantify earthquake hazards in densely populated and rapidly developing regions of eastern Indonesia and provide foundational constraints for studies of resonance frequency.

Production Editor:
Andrea Llenos
Handling Editor:
Vitor Silva
Copy & Layout Editor:
Hannah F. Mark

Received:
October 7, 2024
Accepted:
June 11, 2025
Published:
November 17, 2025

1 Introduction

Indonesia has a very high seismic flux (Harris and Major, 2016) due its position at the intersection of a convergent triple junction of Earth's three largest plates (Eurasian, Australian, and Pacific). Risk of seismic hazards in Indonesia is exacerbated by the fact it is the 4th most populated country in the world. This overlap of high seismic flux and densely populated urban regions makes most parts of the country susceptible to seismic disasters (Baillie and Milne; Koulali et al., 2016; Martin et al., 2022). The intensity of shaking at any given location is determined partially by distance to the epicenter but also by the degree of local wave amplification. Seismic wave amplification is the result of subsurface variables such as vertical and lateral stratigraphic heterogeneity, sediment rheology (soft and hard layers), and geometry of the ground surface (Semblat et al., 2005). Quantifying these risks is essential for establishing evidence-based city zoning laws and reducing losses in future earthquakes. Many of Indonesia's major cities and populous areas are built on poorly consolidated sediment in coastal plains, which increases the threat of wave amplification.

Current structural design codes created by the National Earthquake Hazards Reduction Program

(NEHRP) categorize seismic site effects by classifying them according to the time-averaged shear wave velocity to 30 m depth, a value referred to as V_{s30} (NEHRP, 2015; Council, 2018). The concept of V_{s30} was developed in response to the observation that earthquake damage and loss of life is most severe at sites with unconsolidated fine-grained strata and soft soil conditions, where shear wave velocity is low. Analysis of borehole and strong-motion data associated with the 1989 Loma Prieta earthquake found that mean peak horizontal acceleration, velocity, and displacement are inversely correlated with mean shear wave velocity (Borcherdt and Glassmoyer, 1992; Borcherdt, 1994). Thus, estimates of site response and seismic amplification can be generated by measuring near-surface shear-wave velocity through Multichannel Shear Wave Analysis

Assigning areas with similar seismic hazard risk to site classes aids communities and governments in making seismic zoning maps that can help mitigate potential damage to infrastructure and homes. The BMKG (Indonesia's Meteorology, Climatology, and Geophysical Agency) has previously measured $V_{\rm s30}$ values across Indonesia, but very few measurements exist for eastern Indonesia. The most detailed $V_{\rm s30}$ map available for Indonesia was produced by correlating BMKG reference

values with slope angle across the country, rather than by direct measurement (Irsyam et al., 2017). While this approach provides baseline values for expected V_{s30} in each region, it is still only an approximation of true V_{s30} values and lacks detail.

This study seeks to map zones of likely seismic wave amplification in four densely populated coastal regions in eastern Indonesia: Pacitan (East Java), Lombok, Banda Islands, and Ambon (Figure 1). The locations provide a representative sample of a mature continental arc (Java), nascent continental arc (Lombok), recently extinct oceanic arc (Ambon), and active oceanic arc (Banda). Resulting V_{s30} maps are then compared with Modified Mercalli Intensity (MMI) values, which are semi-quantified earthquake damage observations. The results help address the critical issue of who is most at risk of earthquake-induced ground shaking in eastern Indonesia.

1.1 Geologic Setting: Pacitan City, Java

The city of Pacitan, located in East Java Province (Figure 1), is a coastal community facing south towards the Sunda Trench. Most of the city's population is located on a flat coastal floodplain of the Maron River composed of alluvium and surrounded by hills underlain by bedrock. All but one of this study's sites in Pacitan fall on alluvium. The exception is located on the Arjosari Formation, which consists of polymictic conglomerate, sandstone, siltstone, limestone, claystone, sandy marl and pumiceous sandstone, intercalated with volcanic breccia, lava, and tuff (Samodra et al., 1992).

1.2 Geologic Setting: Lombok Island

The island of Lombok, located in West Nusa Tenggara Province (Figure 1), is an active volcanic arc island mounted on older volcanic material (Eocene-Oligocene). The arc is bounded by thrust faults with opposing vergence. To the south is the north-dipping Sunda subduction zone and to the north is the southdipping Flores Thrust (Figure 1). Most of the island's bedrock is volcanic, associated with its active volcano, Rinjani. Many of this study's sites on Lombok fall on the Lekopiko Formation, a volcanic bedrock consisting of pumiceous tuff, laharic breccia and lava flows. Small volcanic islands can be found off the coasts of Lombok, such as Gili Trawangan, which is dominated by the Kalipalung Formation (alternating calcareous breccia and lava). Flows from Mount Pusuk and Mount Nangi contribute to undifferentiated deposits on the east slope of Mount Rinjani. Sedimentary rocks crop out at the south end of Lombok Island and intermingle with volcanic deposits in units such as the Pengulung Formation. Additionally, coastal plains on the island are underlain by alluvium. The largest alluvial plains on Lombok are located on the west coast, beneath the provincial capital city of Mataram (Andi Mangga et al., 1994).

1.3 Geologic Setting: Banda Islands

The Banda Islands (Figure 1) expose the summit peaks of a large volcanic edifice that rises 5800m above the

Banda Sea floor. These islands are composed of undifferentiated volcanic units. The central Banda Islands comprise an active volcano surrounded by the remains of a larger collapsed caldera. The outer Banda Islands are composed of volcanic and coralline bedrock. This study collected data on 4 islands and spans three geologic units: alluvium, coralline limestone (terraceforming with intercalations of calcareous tuff), and volcanic breccia (andesite to basalt with tuff) (Agustiyanto et al., 1994). The relatively high elevation of the terraces indicates that they are tectonically uplifted, not merely the result of eustatic sea level change.

1.4 Geologic Setting: Ambon Island

Like other inner Banda Arc islands, Ambon (Figure 1) is largely composed of island-arc volcanic rock, though it no longer has active volcanoes. Occasional outcrops of metamorphic and locally ultramafic rock are also present (Pownall et al., 2013; Pownall and Hall). Ambon's metamorphic rocks were exhumed 16 Ma ago by a series of WNW- ESE detachment faults abutting hot mantle lherzolite against the base of the crust (Pownall et al., 2017). This extension not only affected Ambon, but other nearby islands as well, including the island of Seram. According to the geologic map by Tjokrosapoetro et al. (1993), this study's sites on Ambon span four units: alluvium and coralline limestone along with various volcanic units. The Ambon volcanics are characterized as andesite, dacite, breccia, and tuff, while identified mafics and ultramafics on the island include harzburgite, dunite, serpentinite, and gabbro.

2 Methods

2.1 V_{s30} Mapping

This study uses V_{s30} measurements as a proxy for estimating potential seismic wave amplification. Determining V_{s30} consists of four steps: field acquisition of seismic data, processing of data to extract a dispersion curve of phase velocity versus frequency, inversion of the dispersion curve to plot depth versus shear-wave velocity, and calculation of V_{s30} based on the velocity profile model. Seismic data was gathered by conducting MASW surveys for each site within a larger study area. Data acquisition sites were chosen in places that were flat, were large enough for a 50m array of geophones, and had low background noise, such as sports fields.

MASW is a seismic survey technique used to acquire information about the elastic properties of near-surface rock and sediment by analyzing how Rayleigh waves travel through the ground (Park et al., 1999). Each survey deployed twenty-four 4.5-Hz geophones with a receiver spacing of 2.6 m. A 10kg sledgehammer blow to a metal plate acted as the source for the seismic wave with a nearest-receiver offset of 15.7 m. Similar surveys were conducted in several places with a high seismic flux that are densely populated (see review in Foster et al., 2019).

Active MASW data were acquired at each site by taking three surveys at the same location. Each survey was composed of five field-stacked shots. Data were

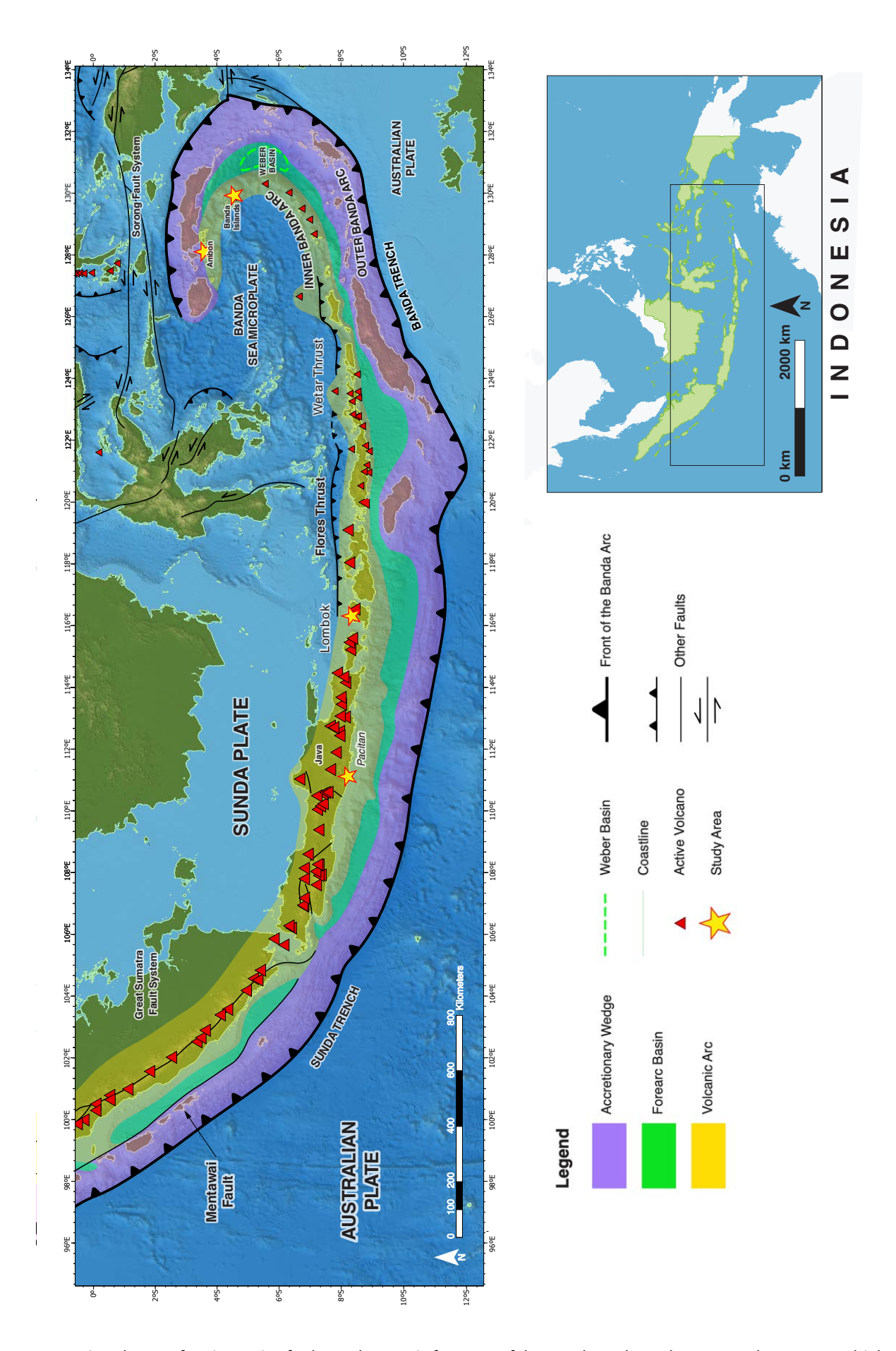


Figure 1 Regional map of major active faults and tectonic features of the Sunda and Banda arc-trench systems, which result from the subduction of the Australian plate beneath the Asian plate. Yellow stars are study areas in a) Pacitan (Java) and Lombok, and b) Banda Islands and Ambon.

recorded with a sampling interval of 0.5 ms and a record length of 2 s for each shot. Passive MASW measurements were also taken at each site, using ambient seismic noise. Passive data were acquired from a stack of three shots with a sampling interval of 2000 ms and a recording time of 30 s. However, most sites did not have enough noise to produce significant dispersion curves, so passive data were not used in the final calculations. Similar surveys were conducted in several places with a high seismic flux that are densely populated (see review in Foster et al., 2019).

MASW data were imported into ParkSEIS. A Rayleigh-wave dispersion image, dispersion curve, and 1-D velocity profile were produced from the data taken at each site and are presented in Supplemental Materials. Percent fit was also calculated to analyze how well actual data compared with simulated "ideal" data.

2.2 Recent Earthquakes and Modified Mercalli Intensity (MMI) Mapping

MMI is a qualitative scale for the intensity of earthquake shaking observed through the extent of damage to the environment, both natural and man-made (Wood and Neumann, 1931; Stover and Coffman, 1993). We utilize previously acquired intensity data and intensity data acquired by us. Specifically, this study incorporates MMI estimates (from prior studies and interviews conducted in conjunction with this study) for recent instrumental earthquakes on Lombok and Ambon and from a well-documented historical event on Ambon in 1898 with calculated V_{s30} data to compare site properties to response.

In 2018, four deadly earthquakes impacted the NW region of Lombok Island in less than a month. The magnitudes were Mw 6.4 on 28 July, Mw 6.9 on 5 August, and both Mw 6.2 and Mw 6.9 on 19 August (U. S. Geological Survey, 2018a,b,c,d). Although the 28 July earthquake was the lowest magnitude, its epicenter was closest to a major population center on the west coast of Lombok, and thus the event for which the most detailed MMI estimates were acquired (from 25 separate locations; Irsyam et al., 2018). After the first of these earthquakes,Indonesia's National Center for Earthquake Studies (PuSGeN) produced a table of MMI observations based on questionnaire surveys from northern and central Lombok (Irsyam et al., 2018), these data were used in this study.

The most recent large earthquake in Ambon was a Mw 6.5 event that occurred on 25 September 2019 (U. S. Geological Survey, 2019). The earthquake happened after this study's $V_{\rm s30}$ field work was conducted, so it was possible to gather MMI observations at the same sites as instrumental data. Following the earthquake, Julian Fretha of the Natural Agency for Disaster Countermeasure (BPBD) Kota Ambon conducted interviews with residents to determine MMI using criteria published by the USGS.

While the Ambon 2019 earthquake is associated with mild to moderate damage in cities across the island, a much more severe earthquake of unknown magnitude occurred near Ambon on January 6, 1898. The MMI scale had not yet been developed, so the resulting

damage was documented in photographs and written records from Dutch colonists inhabiting the islands at the time (Djaoeh, 1898; Verbeek, 1898; van Bemmelen, 1900). This study examined those records, along with antique maps and modern satellite imagery, and correlated them to a range of probable MMI ranges for 41 locations around the island (Landsdrukkerij, 1905; Reproductiebedrijf Topografische Dienst, 1925; Valentijn, 1724; Ashcraft, Brigham Young University). This study's MASW sites on Ambon were selected from these 41 MMI locations to allow for direct analysis of site response.

2.3 V_{s30} and NEHRP Site Class Maps

Interpolated V_{s30} maps were produced for each area by plotting V_{s30} values and considering local geology to reasonably extend values across similar geologic units. The exact approach for each area was based on the density of MASW survey locations. For regions with a relatively dense concentration of survey points, V_{s30} values were directly interpolated across the map area using ArcGIS Pro. Alternatively, regions with few to no survey sites relied more heavily on extending interpolated V_{s30} values across boundaries of compositionally similar geologic units. These site class boundaries should be considered approximations in each case, but especially where V_{s30} data are sparse. For example, for Pacitan, we only had one measurement on the Arjosari Formation, which was 629 m/s, so we assign 629 m/s (class B) for areas covered by the formation. The closest parts of the alluvium to this formation are class C, so we designated the class B/C boundary at the contact betweennthe Arjosari and the alluvium. If we had several measurements for one rock body, like the volcanic rocks in Lombok, we would have used the mean of these values to extend into areas without direct measurements. Nevertheless, we advise that the spatial relationships between V_{s30} and MMI on the maps presented herein should only be regarded as meaningful in areas where both data types are well represented.

3 Results

Results for each study location will be presented in a standardized format, beginning with a map showing the number and location of MASW sites. For Lombok and Ambon, MMI data and interpolated maps are introduced after other results. Finally, an interpolated map of V_{s30} values and NEHRP site classifications presented. Tables containing site numbers, latitude and longitude, velocity (m/s), percent fit, and NEHRP site class can be found in the data and code availability section of this paper.

3.1 Pacitan

A total of 14 sites were surveyed in the Pacitan region, as shown in Figure 2. Almost all are located on recent alluvial deposits associated with the Grindulu River. The exception is site P9, which lies on the intermingled sedimentary and volcanic deposits of the Arjosari Formation

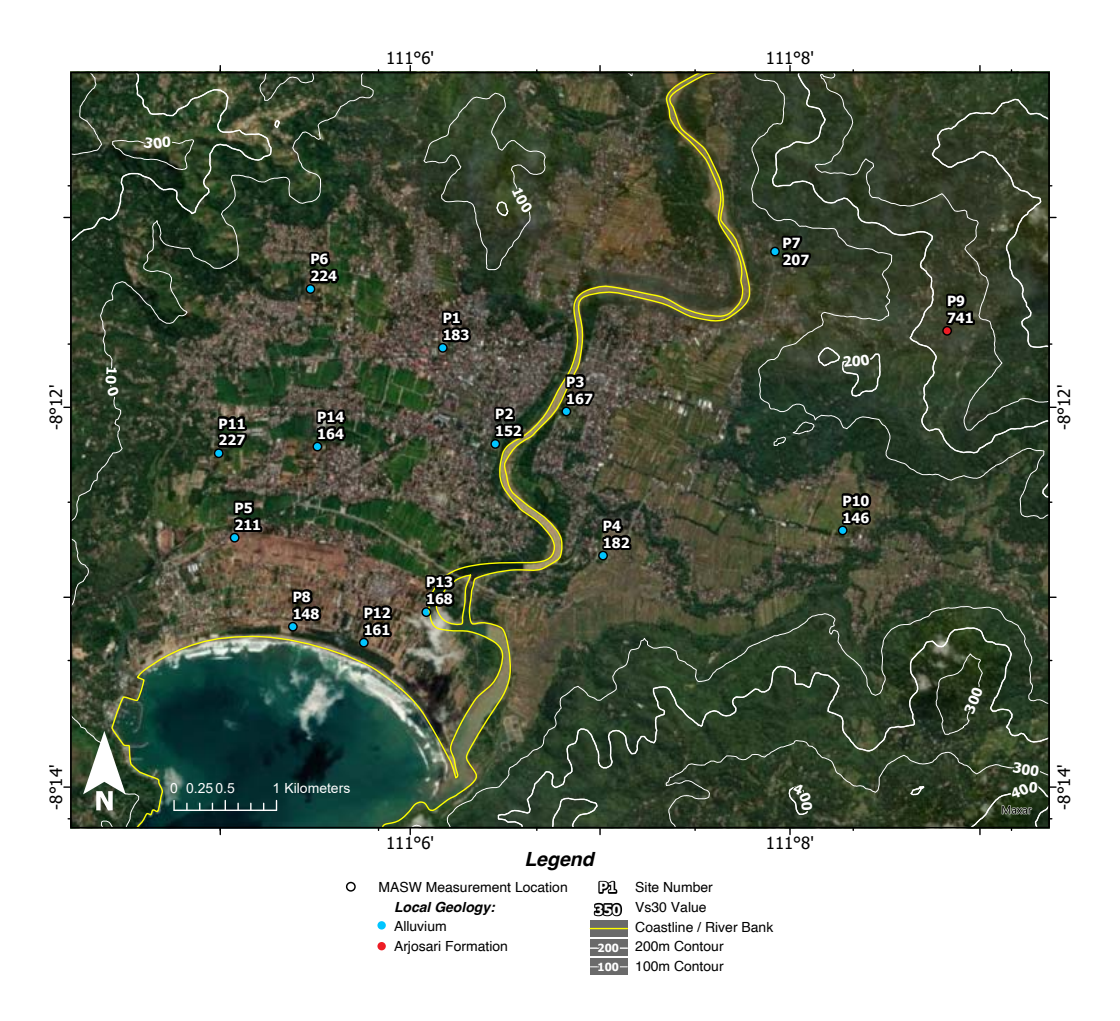


Figure 2 Map of MASW sites surveyed in the Pacitan region. All measurements, except for P9, were taken on the coastal plain, which is the most densely populated part of the city. Elevation contours for all maps shown in this study are sourced from NASA's Shuttle Radar Topography Mission (SRTM) 1-arcsecond topographic rasters, accessible from the USGS Earth Explorer online data portal (U. S. Geological Survey, 2014).

The percent fit between the modeled dispersion curves and the measured dispersion curves at Pacitan ranges from 85 to 98%, though most measurements have a percent fit \geq 95%. Sites with the lowest percent fit between dispersion curves are site P6 (94%), P7 (91%), and P11 (85%). Calculated V_{s30} values range from 148 to 741 m/s.

As a result, NEHRP classifications for Pacitan sites range from C to E (Figure 3). The outlier site of P9 has a V_{s30} of 741 m/s and site class C. All other sites range from 150 to 230 m/s, have a mean V_{s30} of 180 m/s, and fall in site classes D or E. The interpolated site class map is presented in Figure 3. The D zone is closer to the hills while E zones lie at the center of the valley near the bay, though the V_{s30} at P10 (146 m/s) on the eastern end of the valley shows that the E zone may extend farther across the valley. Extents of alluvial deposits in the valley were used to place the boundary between C and D zones. The one measurement located outside the alluvium (P9) is class C and without additional measurements, it is inferred that the surrounding bedrock hills, which have a similar slope to P9, are class C as well.

3.2 Lombok

MASW measurements were acquired from 20 sites on Lombok. The geology of the sites can be broadly sorted into two categories: alluvium and volcanic. Most of the volcanic sites are on the Lekopiko Formation, with the exceptions of L18 and L9. Site L18 overlies undifferentiated volcanic rocks, while Site L9, located on the south side of Gili Trawangan, overlies the Kalipalung Formation (Andi Mangga et al., 1994).

The percent fit between the modeled dispersion curves and the measured dispersion curves ranges from 83 to 98%, with a mean of 94%. Sites with the lowest percent fit between curves are L3 (83%), L9 (87%), L15 (88%), and L18 (88%). The difference in mean percent fit between alluvial sites and volcanic sites was small (94.7% and 93.5%, respectively).

 V_{s30} ranges from 153 to 629 m/s. Site class categorization of Lombok sites range from C to E. The nine V_{s30} measurements on alluvium range from 153 to 261 m/s and have a mean of 212 m/s. Six of these sites fall into NEHRP site class D; the other three class E. All measurements on volcanic units have a V_{s30} >300 m/s except for L12 (243 m/s), and the mean of these 11 measurements is 429 m/s. Seven of these sites fall into class C; the other four are in class D.

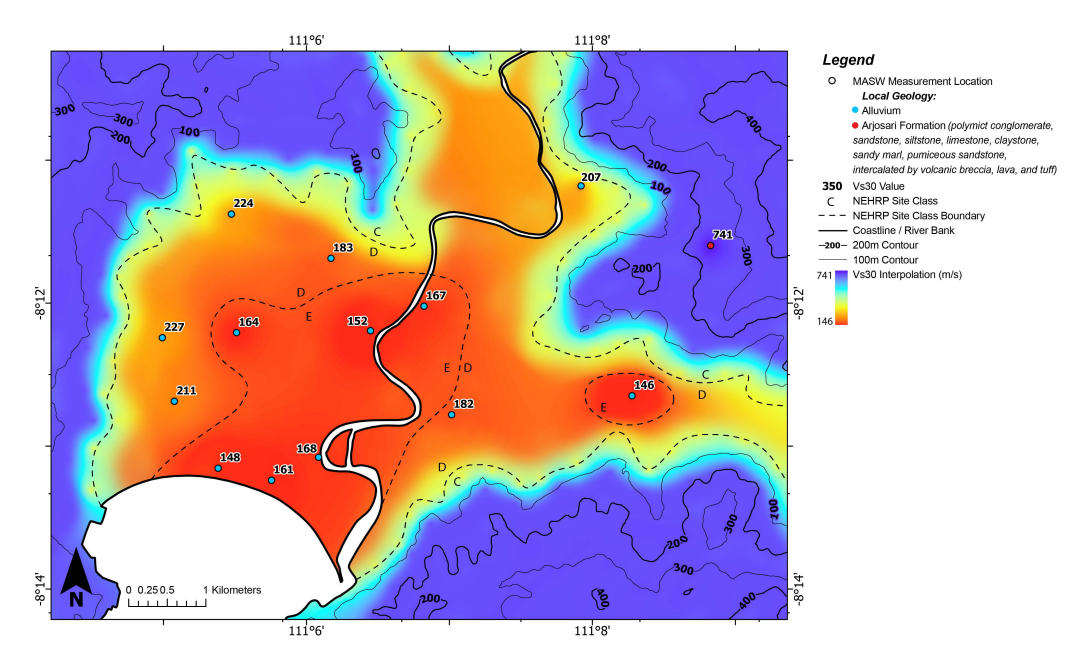


Figure 3 V_{s30} and NEHRP site class map of the Pacitan region. The color gradient represents the interpolation of V_{s30} data points. Interpolation is based on the datapoints as well as data from the region's geologic map (Samodra et al., 1992). Red indicates the regions of lowest V_{s30} while blue indicates the regions of highest V_{s30} .

Using above mentioned MMI data from PuSGeN, a map was produced by assigning coordinates to each observation and interpolating between them (Figure 5). On the northwest side of the island, one alluvial site reported an MMI of 6 while nearby sites reported more consistent values of 4-5. To the northeast, an observation from alluvium recorded MMI=5 while sites on undifferentiated volcanics varied from MMI 6 to 8.

Like Pacitan, NEHRP classes on Lombok range from C to E. All measurements on alluvium are class D or E while those on volcanic rocks are class C or D. Areas in the southern portion of the island were excluded from the interpolation because measurements were not taken directly or on similar geologic units. These classes are interpolated and presented with $V_{\rm s30}$ values in Figure 6.

3.3 Banda Islands

There were nine sites surveyed on the Banda Islands: five on Neira, two on Banda Besar, and one each on Ai and Run (Figure 7). Percent fit between modeled and measured dispersion curves for these sites ranges from 88 to 97%, however all but one have a fit >94%. V_{s30} ranges from 176 to 490 m/s. Alluvial sites have the lowest mean velocity at 230 m/s, though this is skewed by B1's unusually high measurement of 356 m/s. Volcanic breccia sites have a higher mean velocity of 431 m/s, although there are only two such measurements. The single coralline limestone site, on the island of Run, has a V_{s30} of 459 m/s.

The sites surveyed in the Banda Islands range from NEHRP site classes C to E. All volcanic breccia and limestone sites are site class C. Most of the alluvium sites are NEHRP class D, except for B8 on Banda Besar which falls just over the boundary into class E.

3.4 Ambon

The 14 sites surveyed on Ambon are mapped in Figure 9. Seven sites are located on alluvium, three on coralline limestone, three on volcanics, and one on ultramafic and mafic rock. Percent fit values for the measurements on Ambon are >95% with the exceptions of sites A1 (87%), A5 (78%), and A6 (92%). $V_{\rm s30}$ across the island ranges from 180 to 660 m/s. Alluvial sites have the lowest average $V_{\rm s30}$ (262 m/s), followed by limestone sites (330 m/s) and volcanic sites (518 m/s). The single site underlain by ultramafic rock has a $V_{\rm s30}$ within the range of the volcanic sites (453 m/s).

MMI maps produced from the two aforementioned earthquakes on Ambon are shown in Figures 10 and 11. The more recent event occurred on September 25, 2019. After conducting interviews with residents, the BPBD Kota Ambon reported that during this event, most locations experienced an MMI of 4-5, but one site along the bay (in the village of Rumah Tiga) recorded an MMI of 7. The result of interpolating these data points is presented in Figure 7. The earlier event took place on January 6, 1898. The magnitude of the earthquake is unknown but likely higher than the 2019 event. Estimated MMI values are significantly higher, as shown in the interpolated map of Figure 8. The greatest amount of damage was recorded in the village of Rumah Tiga and in the city of Ambon proper.

Measured site classes on Ambon fall in NEHRP site class C or D. All alluvial sites are class D. Two of the limestone sites are class D and one is class C. The sites located on volcanic or ultramafic rock are all class C. Figure 12 displays the interpolated $V_{\rm s30}$ and NEHRP map of Ambon Island.

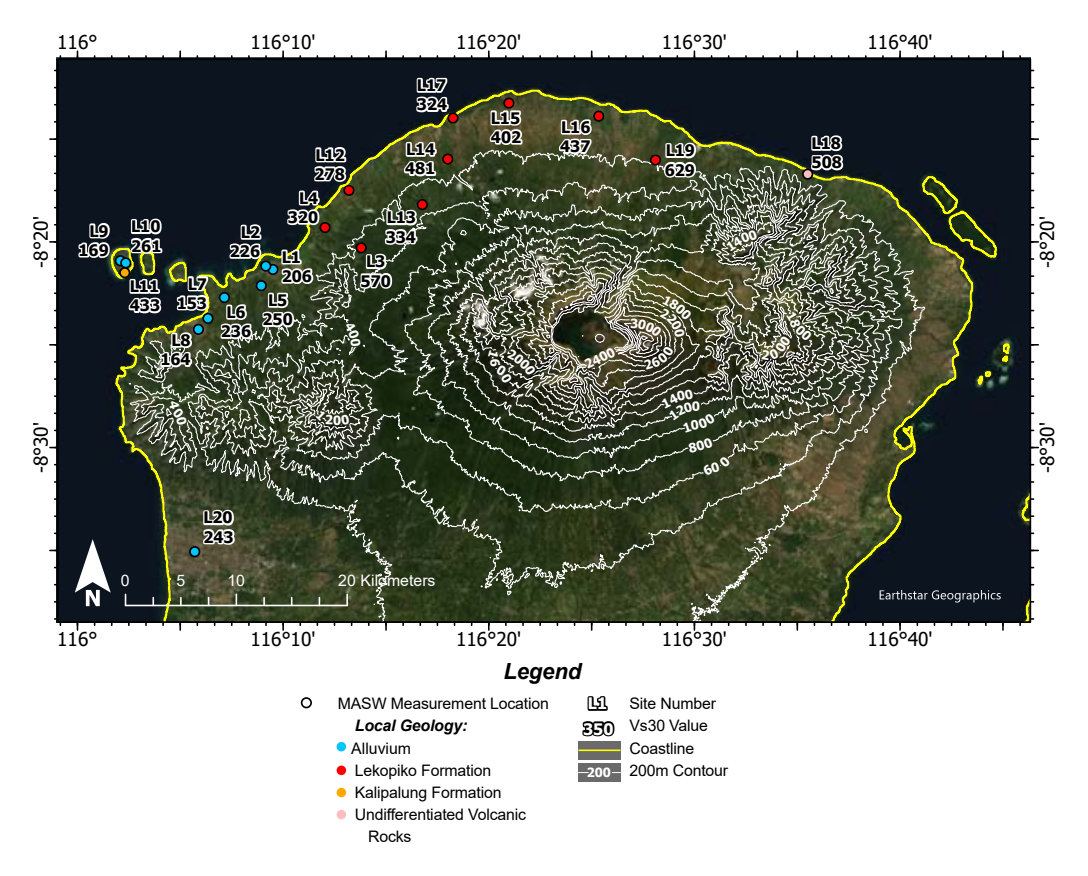


Figure 4 Map of MASW sites surveyed on Lombok. Surveys were focused on the north side of the island, the region most affected by the 2018 earthquakes; however, one measurement was also taken in the center of Mataram city (L20).

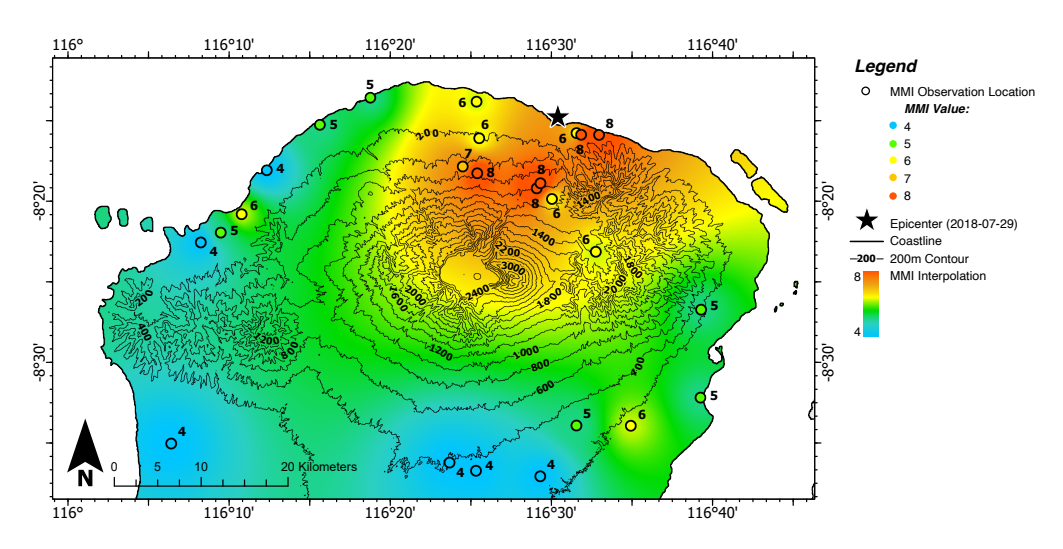


Figure 5 Map of MMI observations on Lombok for the earthquake of July 29, 2018. The epicenter for this earthquake was located on the northern coast and the most severe damage was reported in northeast Lombok. MMI data from Irsyam et al. (2018).

4 Discussion

4.1 Pacitan

The district of Pacitan, which is only slightly larger than the area shown in Figure 9, reported a population of 78,161 in 2020, along with a growth rate of 6.76% from 2010 to 2020 (BPS and Pacitan, 2021). Most people live in the valley, where land is flat and thicker soils make agriculture easier.

While uncertainty remains regarding values as interpolated in Figure 3, this map is valid as a preliminary

estimate of $V_{\rm s30}$ values and NEHRP site classifications until more data becomes available. Placing the boundary between C and D zones along the edges of alluvium is more accurate than a smooth interpolation between the hillside and valley, largely because it takes into account the sudden slope change present at the base of the hills. Large, sudden variance in slope suggests similar variation in $V_{\rm s30}$ values. The alluvial deposits are likely thin and coarse-grained near the mountains, reflected by increased $V_{\rm s30}$ values in these locations. Towards the center of the basin, alluvium is expected to increase

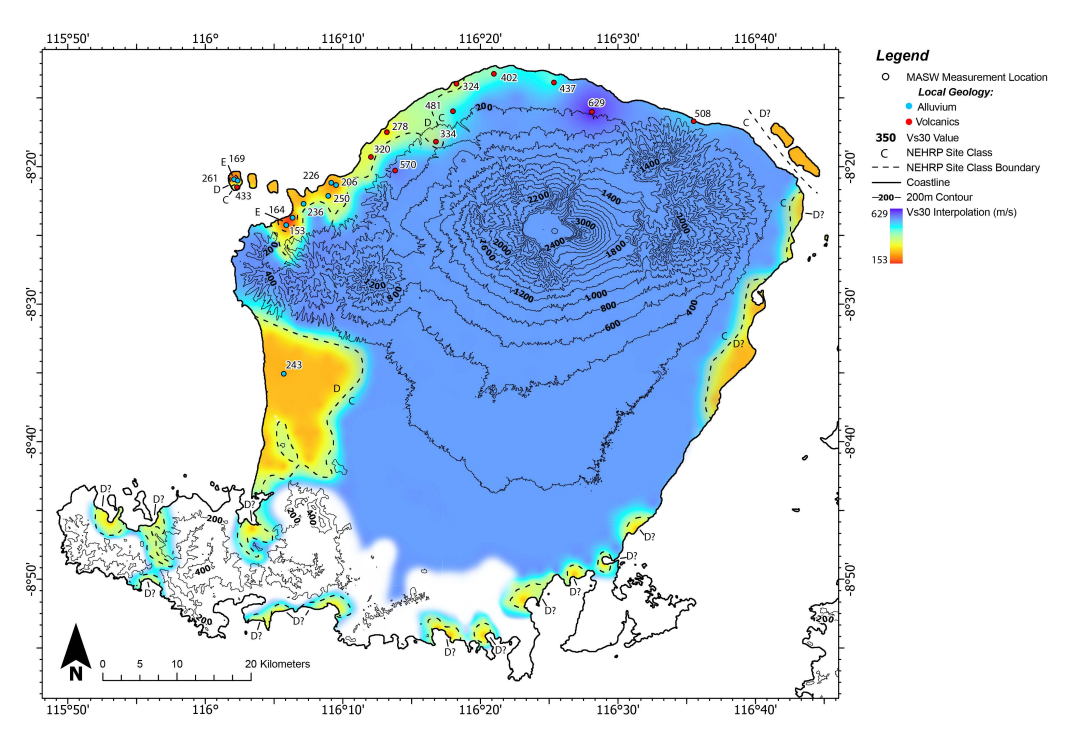


Figure 6 V_{s30} and NEHRP site class map of Lombok. Interpolation is based on the V_{s30} data as well as data from the geologic map (Andi Mangga et al., 1994). Red indicates regions of lowest V_{s30} while blue indicates regions of highest V_{s30} . Areas without shading (white) were excluded from the interpolation, as there were insufficient measurements to infer their potential V_{s30} values. NOte that because we have no V_{s30} data from the interior of the island, the veracity of the interpolation would need to be tested with further field measurements here and other islands studied in this project.

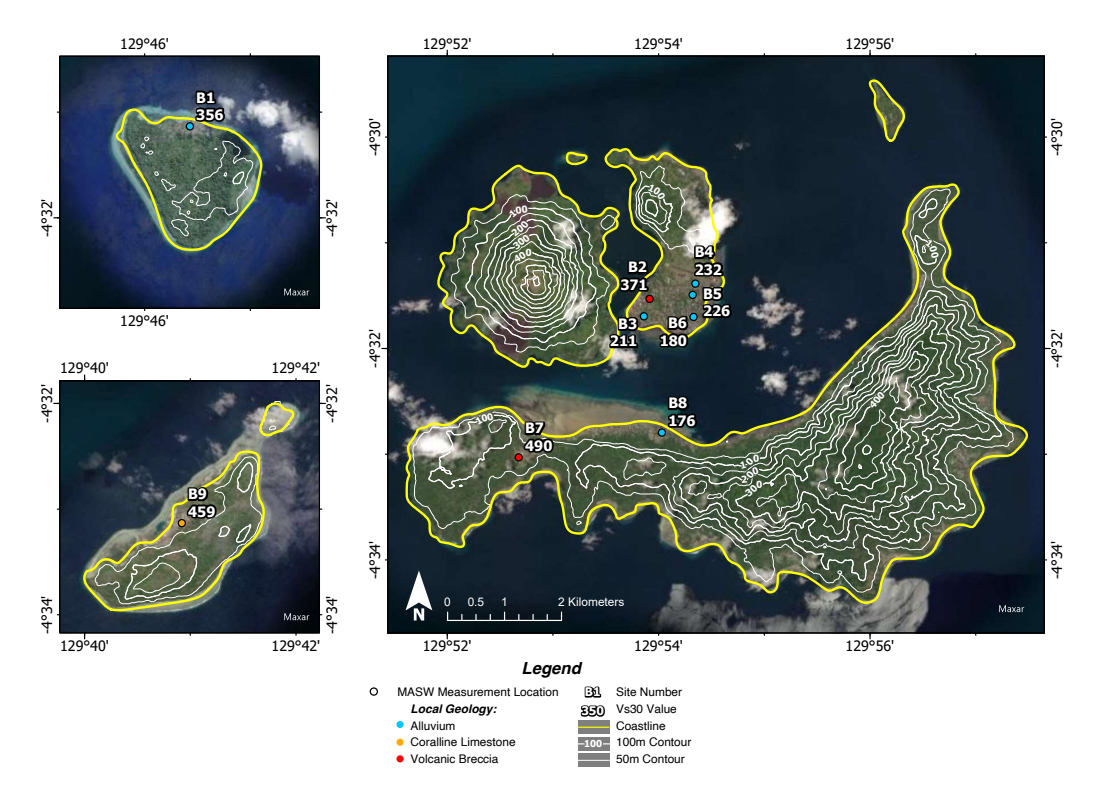


Figure 7 Map of MASW sites surveyed on the Banda Islands. The number of measurements taken was limited by a paucity of flat, open spaces that were accessible and long enough to accommodate the full array of geophones.

in thickness and decrease in grain size, correlated with very low $V_{\rm s30}$ values. It is noted that E zones could have a greater extent in the narrower valleys on both north and east sides of the main coastal plain, but only a few measurements are available in these locations, thus making it difficult to delineate precise boundaries.

Significant uncertainty still exists regarding potential V_{s30} values in the hills due to a lack of data and known variance of geologic units. Non-alluvial units around Pacitan can vary widely in composition, even within a single formation (including the Arjosari formation, where measurement P9 was taken). Lacking compre-

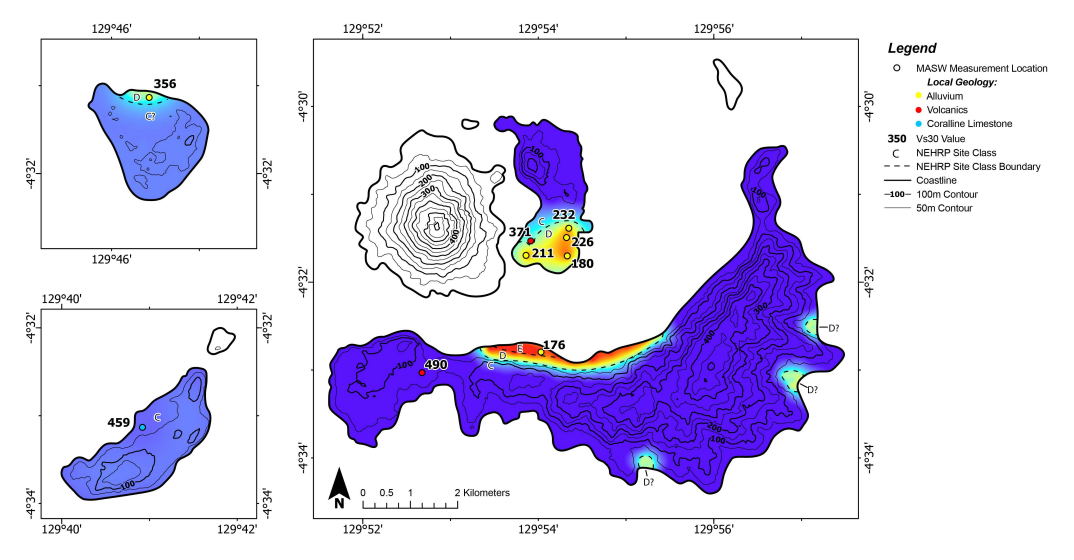


Figure 8 V_{s30} and NEHRP site class map of the Banda Islands. Interpolation is based on the data points as well as data from the region's geologic map (Agustiyanto et al., 1994). Banda Api was excluded from the interpolation as there were no measurements taken on the island. The alluvial deposits on the north side of Banda Besar, the south side of Neira, and the north side of Ai are all class C or D. Alluvial deposits on the south side of Banda Besar may also be class C.

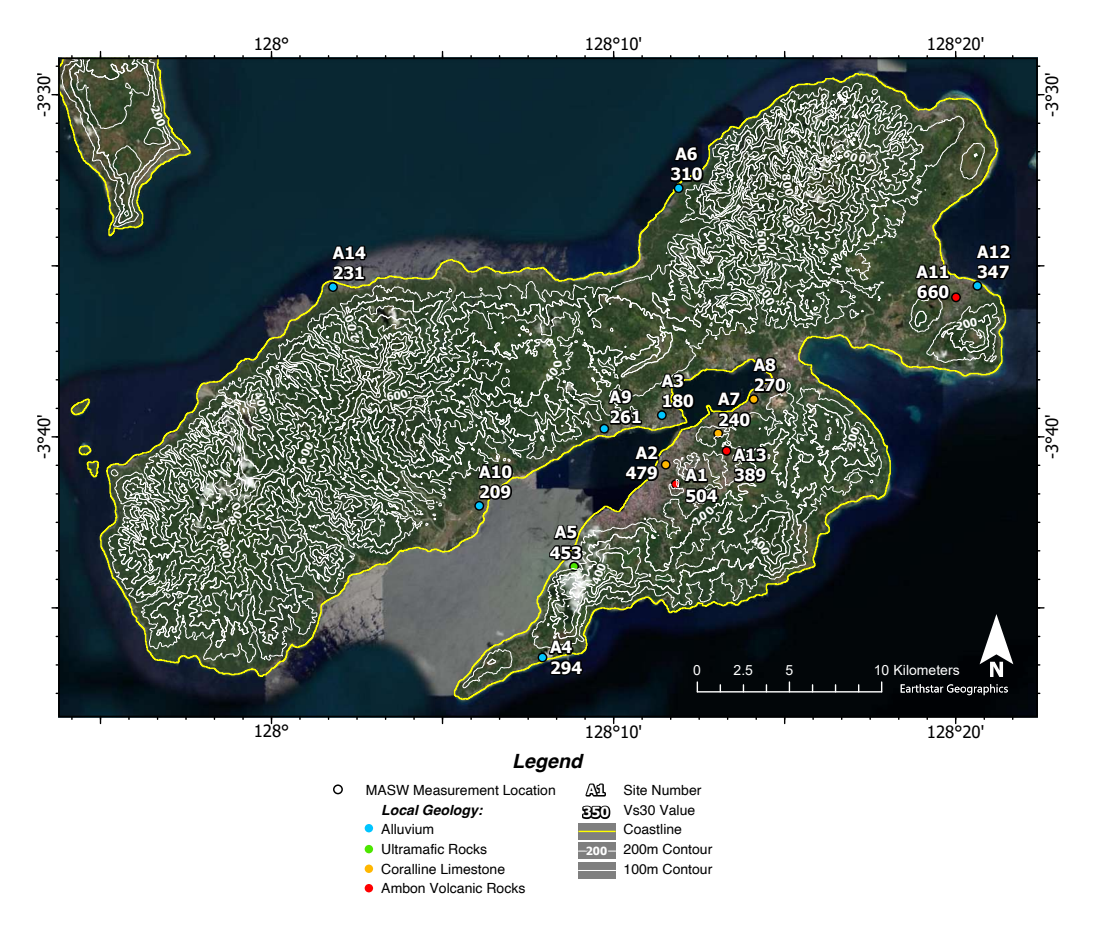


Figure 9 Map of MASW sites surveyed on Ambon. Surveys were concentrated closer to the coast where most of the population is located; most of the inland landscape is mountainous, uninhabited rainforest.

hensive data in the hills, we designate these units as class C.

4.2 Lombok

Measurements were concentrated on the north end of the island, where the impact from the 2018 earthquakes was the greatest, although some sites are on the west coast including one in the city of Mataram. Measurements were taken on three different volcanic units: nine on the Lekopiko formation (278-570 m/s), one on the Kalipalung formation (433 m/s), and one on undifferentiated volcanic rock (508 m/s). The $V_{\rm s30}$ values from the Kalipalung formation and the undifferentiated volcanic formation are within the range of values from the Lekopiko formation, so in the absence of additional

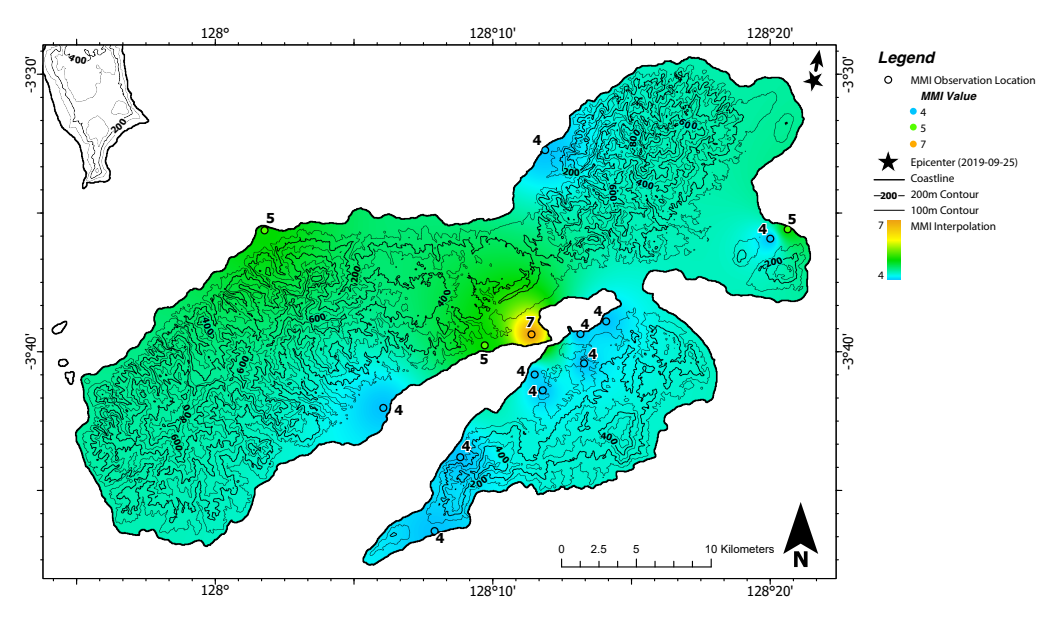


Figure 10 Map of MMI observations on Ambon for the earthquake of September 26, 2019. Damage surveys were conducted by the BPBD Kota Ambon at 14 sites, chosen based on the locations of prior MASW surveys. The epicenter for this event was located at 3.453°S 128.370°E, or 6.5 km northeast of Ambon. The map is shaded using a basic interpolation between the observation points.

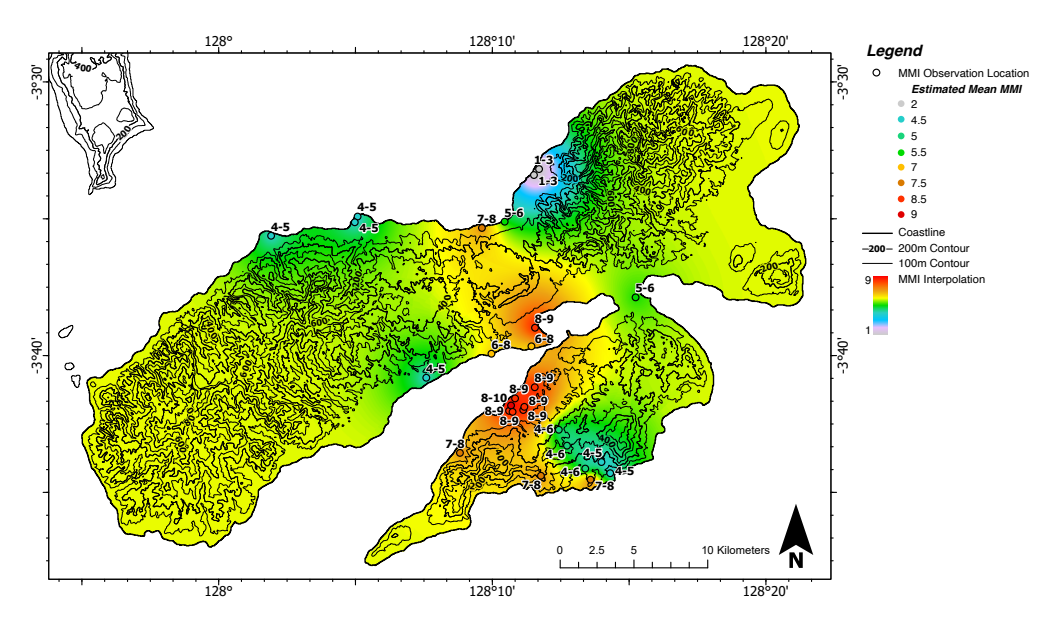


Figure 11 Map of MMI observations on Ambon for the earthquake of January 6, 1898. The epicenter for this event is unknown as it took place before instrumental earthquake records. MMI ratings were determined based on reported damage at 27 different sites around the islands from Djaoeh (1898), Verbeek (1898), and van Bemmelen (1900).

data, these units are treated as the same from an earthquake hazard perspective. It is also reasonable to infer that unmeasured igneous units, such as the Kalibabak formation in western and central Lombok, have similar site classifications.

Similarly, it is inferred that unmeasured alluvial regions on Lombok are class D and could be class E in certain areas. While the alluvial plain on the northwest side of the island has the greatest concentration of low- V_{s30} measurements in this study, this does not necessarily mean that it has the highest risk of earthquakegenerated human casualties. Lombok's largest alluvial plain is located to the west, beneath the city of Mataram and its surrounding urban area. This city alone had a population of 429,651 in 2020, presenting a high risk of

significant human impact should a future earthquake occur closer to this part of the island (BPS and Barat, 2020). In some areas of the Mataram coastal plain, up to 22% of the buildings were damaged during the 2018 earthquake cluster (Septiadhi et al., 2024). Additional, smaller alluvial deposits exist on the south and east sides of the island.

In general, MMI observations closest to the epicenters of the 2018 earthquakes display greater intensities, however there are some discrepancies between gathered data and local geology (including associated $V_{\rm s30}$ values). These discrepancies could be due to several factors. The first is that the MMI observations may not be reliable. The MMI values for the July 29 event were determined by a combination of methods, including di-

rect observations of damage as well as surveys with residents (Irsyam et al., 2018). The level of uncertainty regarding these values cannot be quantified as Irsyam et al. (2018) did not describe the methodology for the MMI survey in detail. If different areas were visited and described by many separate observers, inconsistencies in the way individuals discern and describe damage could affect the accuracy of the overall MMI map.

If the MMI is in fact reliable, another potential explanation is that the local geology is not yet mapped well enough. There is only one geologic map for the island of Lombok as a whole. While 1:100,000-scale geologic maps of individual regencies exist for some parts of Indonesia, the highest resolution map available for Lombok is 1:250,000, which limits the precision of mapped unit contacts. Additionally, units that have been mapped on Lombok are at times classified as undifferentiated or combine several different rock types. If these rock types have separate geophysical properties, the strength of correlations between units and MMI may be reduced.

Along with MMI observation and geologic map accuracy, irregularities in the propagation of earthquake energy as it passes through heterogenous bedrock could contribute to unexpectedly high or low MMI in different areas. Interpreting the shaking of the July 29 event through the lens of site response assumes that the energy of the earthquake radiated homogeneously from the hypocenter. This is likely not the case, and while this simplified approach can be used to understand earthquake energy propagation in some scenarios, the MMI outliers of this event may indicate that a more sophisticated approach is required here.

Finally, the discrepancies between MMI and V_{s30} could be explained by additional variables besides V_{s30} that may impact site response. To determine the efficacy of V_{s30} as a single proxy for predicting site response, a recent study by Gobbi et al. (2020) simulated the effects that a variety of earthquake records had on randomly generated soil profile models. Using V_{s30} alone they struggled to predict earthquake amplification at a site over the entire frequency range and propose the addition of other proxy variables. The addition of these variables to future studies of Lombok could prove to resolve remaining discrepancies.

4.3 Banda Islands

Comparing site classifications to local geology leads to the assumption that land on the Banda Islands underlain by volcanic and limestone deposits across the islands are likely class C, and those underlain by alluvium are class D to E. Most alluvial deposits of significant size have at least one measurement to support this, except for three small areas of alluvium on the south and east sides of Banda Besar.

With surficial deposits on Banda Api composed of thick volcanic ash layers and very young lava flows, it is possible that surveys taken here produce $V_{\rm s30}$ values that are dissimilar to those associated with older volcanic deposits on other islands. Without direct measurements, this study lacks data to infer site classifica-

tions on Banda Api. The smallest, uninhabited islands in the archipelago were also excluded.

4.4 Ambon

While no site on Ambon had a velocity within the range of Class E (defined as <180 m/s), the low velocities of alluvial sites A3 and A10 (180 and 209 m/s, respectively) are close enough to the site class boundary that class E zones could also exist at as-of-yet unmeasured sites on Ambon's alluvial plains. This would align with the surveys in Pacitan, Lombok, and the Banda Islands, all of which have class E zones near the coast over deposits of alluvium.

Unlike Pacitan or Lombok, however, two of Ambon's measurements were located at sites with coralline limestone bedrock. While limestone only accounts for a minor part of the total surface area of the island, Ambon has many individual mapped exposures, and those surveyed produced V_{s30} values corresponding to classes C and D. This suggests that structures built on limestone bedrock may need to be constructed to a higher standard than those built on volcanic bedrock. However, both class D limestone sites were located close to mapped alluvium as well as the coast. Considering uncertainties associated with unit contacts, it is possible that these two class D sites are located on alluvium rather than limestone, though outcrops were not observed at the site. More MASW measurements at limestone sites would confirm the behavior of Rayleigh waves through Ambon's limestone deposits.

Because Ambon's topography is generally steep, most of its cities are built on the flatter coastal alluvium. This means that most of the island's 347,288 residents live and work in buildings constructed on class D land (BPS and Maluku, 2020). The most densely populated area of the island is the city of Ambon and its surrounding urban area along Ambon Bay. This is also where the damage was most severe during the 2019 and 1898 earthquakes. In 2019, the highest MMI was 7, occurring in the village of Rumah Tiga. Here, structures are built on alluvium along the strait that separates the inner and outer portions of Ambon Bay. However, in 2019 Ambon City, which is built on alluvium across the strait and to the south, only reported an MMI of 4. Alternately, the 1898 event significantly impacted both Rumah Tiga and the city of Ambon, with recorded damage correlating to MMI observations as high as 10 (Djaoeh, 1898; Verbeek, 1898; van Bemmelen, 1900).

Correlation between MMI of these events and V_{s30} values is strongest in Ambon Bay (near Ambon City and Rumah Tiga). At other locations around the island, this correlation can be more tenuous. For example, site A10, which is located on alluvium on the north side of Ambon Bay, has a V_{s30} of 209 m/s. However, A10's MMI (4) was lower in the 2019 earthquake than the MMI 5 reported at site A9, which has a higher V_{s30} (261 m/s), and much lower than alluvial site A3 (180 m/s; MMI=7). Similarly, on the northeast side of the island, site A12 (347 m/s) recorded an MMI of 5, while on the north side of the island, site A6 (310 m/s) recorded an MMI of 4. The difference between MMI 4 and 5 is minor (creaking

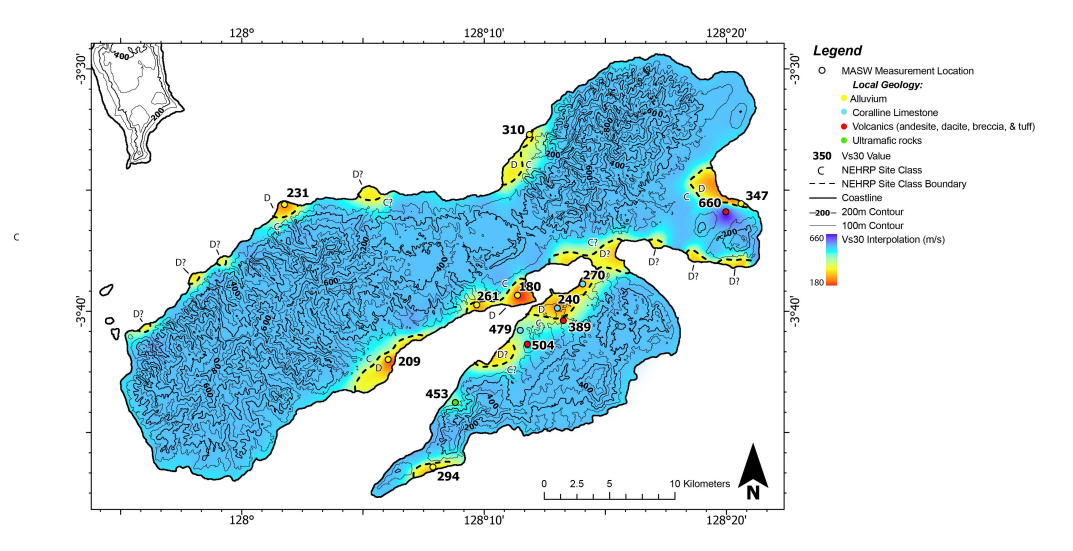


Figure 12 V_{s30} and NEHRP site class map of Ambon. Interpolation is based on the datapoints as well as data from the region's geologic map (Tjokrosapoetro et al., 1993). Red indicates the regions of lowest V_{s30} while blue indicates the regions of highest V_{s30} . See the main text for discussion of which site classes correspond to specific geologic environments.

walls with no damage compared to occasional cracked plaster or windows) but not insignificant. This inconsistency is likely due at least in part to proximity of each site from the epicenter of the earthquake, northeast of the island, though this cannot explain the disparity entirely. Proximity to the epicenter also cannot be used in explaining disparities regarding MMI of the 1898 earthquake, as its epicenter is unknown, but the disparities themselves can still be discussed.

Due to the 1898 event, villages located on deltas on the north side of the island described damage consistent with an MMI of 4-5. One such delta has a $V_{\rm s30}$ value of 231 m/s (Site A14). This is comparable to site A9, though this area saw damage corresponding to MMI of 6-8. The south side of the island also reported unexpectedly intense damage (7-8), particularly near site A5, which has a high $V_{\rm s30}$ at 453 m/s. Again, this could be due to closer proximity to the epicenter, but without instrumentation it cannot be known for certain.

Apart from proximity to the epicenter, the issues in correlating MMI that were encountered with Lombok must also be addressed for Ambon. The MMI observations for the 2019 event were collected by one group from Ambon's BNPB, so inaccuracies or inconsistencies among those observations are unlikely. These observations were also collected at the same sites where MASW surveys were conducted, allowing for V_{s30} and MMI to be directly compared despite limited and potentially misplaced geologic data and unit contacts for Ambon. Thus, the most likely factors that may contribute to unexpected MMI observations are again heterogeneous scattering of earthquake energy and other unmeasured variables.

5 Broader Impacts

Like in most V_{s30} studies, the areas with the lowest V_{s30} values were flat coastal plains filled with unconsolidated alluvium. This corroborates previous research that has correlated decreasing slope angle to decreasing V_{s30} (Wald and Allen, 2007; Allen and Wald, 2009).

Stronger, more consolidated rock is associated with higher shear-wave velocities, while its increased competency allows this rock to maintain steeper slopes. Unconsolidated sediment, in contrast, corresponds with low velocities. This material is more likely to be deposited at low gradients and under lower energy conditions rather than accumulating on steep hillsides (Park and Elrick, 1998). At each of the regions surveyed, the population density is highest on low-lying alluvial deposits with low $V_{\rm s30}$ values.

The risk associated with large populations living on low-velocity alluvial plains can be compounded by other geologic hazards. For example, in northwest Lombok, a vertical tsunami evacuation shelter was constructed on alluvium prior to the 2018 earthquakes. This structure was intended for use in the event of a tsunami to accommodate evacuees who would otherwise not be able to reach high ground in time. When the earthquakes struck northern Lombok, the stairways for the shelter collapsed, rendering it useless. Luckily a tsunami did not follow the earthquakes, but if it had, the casualties associated with building on low-velocity sediment would have extended beyond structural damage to homes, schools, and workplaces.

5.1 Risk Reduction

The findings of this study highlight the importance of improving Indonesia's structural resilience against earthquakes. While addressing structures in alluvial areas with low $V_{\rm s30}$ is most critical, the events discussed here demonstrate that even those built in higher $V_{\rm s30}$ areas would benefit from reinforcement. In Indonesia, buildings constructed of unreinforced masonry and topped with heavy tile roofs are abundant. Indonesia's status as a developing country and a lack of seismic building code enforcement makes these structures all the more common. A change in building style is necessary to mitigate earthquake hazards.

Costa Rica, another developing country with a tropical climate and the potential for large earthquakes, has



Figure 13 Photographs of (A) a school destroyed by the 2018 Lombok earthquake series, and (B) a bamboo school built after the earthquakes. Teachers struggled to get students to attend school in the new building due to its construction style.

found significant success mitigating earthquake hazards through steel reinforcement. Here, buildings are often built of steel, steel-reinforced concrete, or steel-reinforced masonry. Additionally, construction with materials such as adobe, rammed earth, or unreinforced masonry is prohibited (CFIA, 2011; Gutiérrez, 2015). Although Costa Rica's gross national income per capita is higher than Indonesia's, the significant benefits of adopting Costa Rican building practices warrant further exploration and potential implementation by the Indonesian government.

6 Conclusions

Indonesia has a history of large earthquakes that have caused significant damage to structures and many human casualties. Understanding which areas are most susceptible to intense shaking in a future earthquake allows disaster mitigation authorities to know where to focus their main efforts. The purpose of this study was to map $V_{\rm s30}$ for seismically vulnerable regions of Indonesia where it had previously never been measured and use these data, in conjunction with known geology and MMI observations, to identify areas where the risk of structural damage is highest.

In all four study areas (Pacitan, Lombok, Ambon, and

the Banda Islands), the lowest $V_{\rm s30}$ values are found on low-lying, relatively flat coastal alluvial deposits. These correspond with NEHRP site classes D to E. Most non-alluvial survey sites are underlain by volcanic rock, and there is generally not a significant difference between the ranges of $V_{\rm s30}$ values across different volcanic formations. These sites are typically class C, though a few class D sites are identified.

When comparing the calculated V_{s30} values to MMI maps of earthquakes on Lombok and Ambon, discrepancies are observed that cannot entirely be explained by proximity of the observation sites to the epicenters. There are several possible explanations for this, such as insufficient geological mapping or heterogeneous scattering of earthquake energy. Increasing the number of V_{s30} survey sites, and for the case of Lombok, conducting surveys in areas where MMI observations were recorded, may help clarify these differences. Clearly, future field seismic measurements are needed in the interiors of the islands studied to establish better the correlation between earthquake phenomenology and surface geology, V_{s30} , and MMI.

While the measurements from this study act as foundational work for understanding V_{s30} variability in the areas surveyed, these results set the stage for using approaches such as horizontal-to-vertical spectral ratio (HVSR) in future work. This method determines the dominant shaking frequency and shear wave velocity gradient at each site. The measurements also require less equipment and less time. However, a V_{s30} value is required to process the data. Though this study focused on only four areas in Indonesia, virtually any inhabited place in the country could benefit from having these surveys conducted locally.

Acknowledgements

Funding for this research was generously provided through grants from Geoscientists Without Borders, which is affiliated with the Society of Exploration Geophysicists (SEG). In Harm's Way non-profit organization (inharmswayhelp.org) and Brigham Young University also provided funds. We thank Universitas Pembangunan Nasional (UPN Jogjakarta) who sponsors our research in Indonesia. We express appreciation for logistical assistance from the BPBD and governor's offices of Pacitan, Mataram, Banda Islands and Ambon. We are grateful for the logistical coordination and help of Deborah Harris and Poliman Harsono. We also acknowledge the help of Marcell Brown, Schipper Clawson and Roland Lee. We appreciate the reviews by five anonymous referees, which greatly improved the final version of the paper.

Data and code availability

Supplementary materials are available online through figshare.

 V_{s30} Data Tables: Ashcraft et al. (2024a).

MASW Dispersion Curves (derived products from raw MASW collected by the authors): Ashcraft et al. (2024b).

Raw and digital MASW data can be made available upon request to Dr. John McBride at Brigham Young University (mcbseis@gmail.com).

Raw and digital MMI data collected by the authors specifically for this study: Baginski et al. (2024).

ParkSEIS code was used for analysis; code data is not available but resources containing information pertaining to that code can be found at https://www.parkseismic.com/. Other questions can be directed to Dr. John McBride at Brigham Young University (mcbseis@gmail.com).

Competing interests

The authors have no competing interests.

References

- Agustiyanto, D. A., Suparman, M., Partoyo, E., and Sukarna, D. *Peta Geologi Lembar Moa, Damar dan Bandanaira*. Maluku. map, Bandung, Jawa Barat; Pusat Penelitian dan Pengembangan Geologi, 1994.
- Allen, T. I. and Wald, D. J. On the Use of High-Resolution Topographic Data as a Proxy for Seismic Site Conditions (VS30). Bulletin of the Seismological Society of America, 99(2A):935–943, Apr. 2009. doi: 10.1785/0120080255.
- Andi Mangga, S., Atmawinata, S., Hermanto, B., Setyogroho, B., and Amin, T. C. Peta Geologi Lembar Lombok, Nusatenggara Barat. map, Bandung, Jawa Barat; Pusat Penelitian dan Pengembangan Geologi. 1994.
- Ashcraft, C., Harris, R., Fretha, J., Mangam, A., McBride, J., Prasetyadi, C., Rey, K., Orme, S., Baginski, E., Sulaeman, H., Agustinawati, D., Berrett, B., Willmore, R., Bell, I., Westfall, E., and Pradipta, G. C. Vs30 Tables— Ashcraft et al. 2024. 7 2024a. doi: 10.6084/m9.figshare.26210507.v1.
- Ashcraft, C., Harris, R., Fretha, J., Mangam, A., McBride, J., Prasetyadi, C., Rey, K., Orme, S., Sulaeman, H., Agustinawati, D., Berrett, B., Willmore, R., Westfall, E., and Bell, I. Supplemental Materials: Earthquake Shaking Intensity Estimates (Vs30) of Coastal Cities in Eastern Indonesia. Claire Ashcraft et al. 7 2024b. doi: 10.6084/m9.figshare.26156146.v1.
- Ashcraft, C. E. Field Investigations and Numerical Modeling of Earthquake and Tsunami Risk at Four Vulnerable Sites in Indonesia. Master's thesis, Department of Geological Sciences, Brigham Young University, Brigham Young University.
- Baginski, E., Ashcraft, C., Harris, R., Fretha, J., Mangam, A., McBride, J., Prasetyadi, C., Rey, K., Orme, S., Sulaeman, H., Agustinawati, D., Berrett, B., Willmore, R., Bell, I., Westfall, E., and Pradipta, G. C. Supplemental Materials (MMI Data): Earthquake Shaking Intensity Estimates (Vs30) of Coastal Cities in Eastern Indonesia. Claire Ashcraft et al. 2024. 10 2024. doi: 10.6084/m9.figshare.27184008.v1.
- Baillie, P. and Milne, C. New Insights Into Prospectivity and Tectonic Evolution of the Banda Arc: Evidence from Broadband Seismic Data. In *Proc. Indonesian petrol. Assoc., 38th Ann. Conv.* Indonesian Petroleum Association (IPA). doi: 10.29118/ipa.0.14.g.100.
- Borcherdt, R. D. Estimates of Site-Dependent Response Spectra for Design (Methodology and Justification). *Earthquake Spectra*, 10 (4):617–653, Nov. 1994. doi: 10.1193/1.1585791.
- Borcherdt, R. D. and Glassmoyer, G. On the characteristics of local geology and their influence on ground motions generated by the Loma Prieta earthquake in the San Francisco Bay region,

- California. *Bulletin of the Seismological Society of America*, 82 (2):603–641, Apr. 1992. doi: 10.1785/bssa0820020603.
- BPS and Barat, P. N. T. Statistik Gender Provinsi Nusa Tenggara Barat. Unpublished, 2020.
- BPS and Maluku, P. Potret Sensus Penduduk 2020: Provinsi Maluku. Unpublished, 2020.
- BPS and Pacitan, K. Kabupaten Pacitan Dalam Angka 2021. Unpublished, 2021.
- CFIA. *Código sísmico de Costa Rica 2010*. Editorial Tecnológica de Costa Rica, 2011.
- Council, I. C. 2018 International Building Code. ICC, 728p, 2018.
- Djaoeh, B. *Ambon Vóór en Na de Ramp*. Eigen Haard, 1898.
- Foster, K. M., Bradley, B. A., McGann, C. R., and Wotherspoon, L. M. A VS30 Map for New Zealand Based on Geologic and Terrain Proxy Variables and Field Measurements. *Earthquake Spectra*, 35(4):1865–1897, Nov. 2019. doi: 10.1193/121118eqs281m.
- Gobbi, S., Lenti, L., Santisi d'Avila, M. P., Semblat, J.-F., and Reiffsteck, P. Influence of the variability of soil profile properties on weak and strong seismic response. *Soil Dynamics and Earth-quake Engineering*, 135:106200, Aug. 2020. doi: 10.1016/j.soildyn.2020.106200.
- Gutiérrez, J. Seismic Risk Prevention in Costa Rica: A Successful 39 Year Experience. In *15th World Conference on Earthquake Engineering 2012 (15WCEE)*, pages 29703–29712, Lisbon, Portugal; Curran Associates, Inc, 2015. 37.
- Harris, R. and Major, J. Waves of destruction in the East Indies: the Wichmann catalogue of earthquakes and tsunami in the Indonesian region from 1538 to 1877. *Geological Society, London, Special Publications*, 441(1):9–46, May 2016. doi: 10.1144/sp441.2.
- Irsyam, M., Asrurifak, M., Mikhail, R., Wahdiny, I. I., Rustiani, S., and Munirwansyah, M. Development of Nationwide Vs30 Map and Calibrated Conversion Table for Indonesia using Automated Topographical Classification. *Journal of Engineering and Technological Sciences*, 49(4):457–471, Oct. 2017. doi: 10.5614/j.eng.technol.sci.2017.49.4.3.
- Irsyam, M., Hanifa, N. R., and Djarwadi, D. Kajian Rangkaian Gempa Lombok, Provinsi Nusa Tenggara Barat, 29 Juli 2018 (M6.4), 5 Agustus 2018 (M7.0), 19 Agustus 2018 (M6.9). Pusat Penelitian dan Pengembangan Perumahan dan Permukiman, Badan Penelitian dan Pengembangan, Kementerian Pekerjaan Umum dan Perumahan Rakyat. Unpublished, 2018.
- Koulali, A., Susilo, S., McClusky, S., Meilano, I., Cummins, P., Tregoning, P., Lister, G., Efendi, J., and Syafi'i, M. A. Crustal strain partitioning and the associated earthquake hazard in the eastern Sunda-Banda Arc. *Geophysical Research Letters*, 43(5): 1943–1949, Mar. 2016. doi: 10.1002/2016gl067941.
- Landsdrukkerij. *Kaart van Ambon*. Geologische Beschrÿving van Ambon. map, Batavia, Nederlandsch-Indië, 1905.
- Martin, S. S., Cummins, P. R., and Meltzner, A. J. Gempa Nusantara: A Database of 7380 Macroseismic Observations for 1200 Historical Earthquakes in Indonesia from 1546 to 1950. *Bulletin of the Seismological Society of America*, 112(6):2958–2980, Nov. 2022. doi: 10.1785/0120220047.
- NEHRP. NEHRP Recommended Seismic Provisions for New Buildings and Other Structures (FEMA P-1050-1), volume 1. Building Seismic Safety Council, Washington, D. C., 2015.
- Park, C. B., Miller, R. D., and Xia, J. Multichannel analysis of surface waves. *GEOPHYSICS*, 64(3):800–808, May 1999. doi: 10.1190/1.1444590.
- Park, S. and Elrick, S. Predictions of shear-wave velocities in southern California using surface geology. *Bulletin of the Seis-*

- *mological Society of America*, 88(3):677–685, June 1998. doi: 10.1785/bssa0880030677.
- Pownall, J. M. and Hall, R. Neogene Extension on Seram: a New Tectonic Model for the Northern Banda Arc. In *Proc. Indonesian petrol. Assoc., 38th Ann. Conv.* Indonesian Petroleum Association (IPA). doi: 10.29118/jpa.0.14.g.305.
- Pownall, J. M., Hall, R., and Watkinson, I. M. Extreme extension across Seram and Ambon, eastern Indonesia: evidence for Banda slab rollback. *Solid Earth*, 4(2):277–314, Sept. 2013. doi: 10.5194/se-4-277-2013.
- Pownall, J. M., Forster, M. A., Hall, R., and Watkinson, I. M. Tectonometamorphic evolution of Seram and Ambon, eastern Indonesia: Insights from 40 Ar/ 39 Ar geochronology. *Gondwana Research*, 44:35–53, Apr. 2017. doi: 10.1016/j.gr.2016.10.018.
- Reproductiebedrijf Topografische Dienst. Ambon-Groep. map, Weltevreden, Batavia, Nederlandsch-Indië. Unpublished, 1925.
- Samodra, H., Gafoer, S., and Tjokrosapoetro, S. Peta Geologi Lembar Pacitan, Jawa. map, Bandung, Jawa Barat. *Pusat Penelitian dan Pengembangan Geologi.*, 1992.
- Semblat, J., Kham, M., Parara, E., Bard, P., Pitilakis, K., Makra, K., and Raptakis, D. Seismic wave amplification: Basin geometry vs soil layering. *Soil Dynamics and Earthquake Engineering*, 25 (7–10):529–538, Aug. 2005. doi: 10.1016/j.soildyn.2004.11.003.
- Septiadhi, A., Agustawijaya, D. S., and Zubaidah, T. Microtremor-Based Seismic Vulnerability Characteristics in Mataram City. *RE-SEARCH REVIEW International Journal of Multidisciplinary*, 9(5): 212–220, May 2024. doi: 10.31305/rrijm.2024.v09.n05.026.
- Stover, C. and Coffman, J. Seismicity of the United States, 1568-1989 (revised). 1993. doi: 10.3133/pp1527.
- Tjokrosapoetro, S., Rusmana, E., and Achdan, A. *Peta Geologi Lembar Ambon*. Maluku. map, Bandung, Jawa Barat; Pusat Penelitian dan Pengembangan Geologi, 1993.
- U. S. Geological Survey. EarthExplorer, 2014. https://earthexplorer.usgs.gov/.
- U. S. Geological Survey. M 6.4 33 km NNW of Labuan Lombok, Indonesia, 2018a. https://earthquake.usgs.gov/earthquakes/ eventpage/us2000ggbs/executive.
- U. S. Geological Survey. M 6.9 36 km NW of Labuan Lombok, Indonesia, 2018b. https://earthquake.usgs.gov/earthquakes/ eventpage/us1000g3ub/executive.
- U. S. Geological Survey. M 6.3 19 km NNW of Labuan Lombok, Indonesia, 2018c. https://earthquake.usgs.gov/earthquakes/ eventpage/us1000gcvr/executive.
- U. S. Geological Survey. M 6.9 20 km NNW of Labuan Lombok, Indonesia, 2018d. https://earthquake.usgs.gov/earthquakes/ eventpage/us1000gda5/executive.
- U. S. Geological Survey. M 6.5 33 km NE of Ambon, Indonesia, 2019. https://earthquake.usgs.gov/earthquakes/eventpage/us70005lfd/executive.
- Valentijn, F. De Platte Grond van Amboina, soo als het was inden Jaare 1718. Oud en Nieuw Oost-Indiën. map, Dordrecht, Amsterdam; Joannes van Braam & Gerard onder de Linden, 1724.
- van Bemmelen, W. Natuurkundig Tijdschrift voor Nederlandsch-Indië. Ser., 59, 1900.
- Verbeek, R. D. M. *Kort Verslag Over de Aardbeving te Ambon op 6 Januari 1898.* Batavia Landsdrukkerij, 1898.
- Wald, D. J. and Allen, T. I. Topographic Slope as a Proxy for Seismic Site Conditions and Amplification. *Bulletin of the Seismological Society of America*, 97(5):1379–1395, Oct. 2007. doi: 10.1785/0120060267.
- Wood, H. O. and Neumann, F. Modified Mercalli intensity scale of 1931. *Bulletin of the Seismological Society of America*, 21(4):

277-283, Dec. 1931. doi: 10.1785/bssa0210040277.

The article V_{s30} of Coastal Cities in Eastern Indonesia in the Context of Earthquake Phenomenology © 2025 by Claire Ashcraftis licensed under CC BY 4.0.